Free-Flight Investigations of Subliming Ablators and Transpiration Cooling at Hypersonic Velocities

THOMAS E. WALTON JR., * BERNARD RASHIS,† AND CLYDE W. WINTERS‡
NASA Langley Research Center, Hampton, Va.

The results of several free-flight investigations, in which the thermal protection was provided either by a subliming ablator or by transpiration cooling, are discussed. The flight-test regime covered an altitude band from about 177,000 to 25,000 ft and peak velocities ranged from 3900 to 22,200 fps. The similarities between subliming ablators and transpiration cooling are described, and it is shown how the effectiveness of ablation materials can be predicted accurately from transpiration data. This analytical procedure permits direct comparison of the two types of heat protection and allows extrapolation, based on low-speed transpiration data, of ablation material effectiveness to supercircular velocities.

Nomenclature

c_p = specific heat, Btu/lb-°F
F = ratio of coolant mass-flow rate to local air mass-flow rate
F_ξ = nondimensional coolant flow rate, $w/S(\rho V)_2$
f = fraction of vaporization
H = enthalpy, Btu/lb
h_{eff} = effective heat of ablation, Btu/lb
h_{ov} = material intrinsic heat capacity, Btu/lb
$\dot{m}$ = ablation rate, psf-sec
n = temperature ratio exponent
N_{St} = Stanton number
q = heat-transfer rate, Btu/ft²-sec
S = cooled area downstream of porous nose, ft²
T = temperature, °R
w = coolant flow rate, lb/sec
V = velocity, fps
ρ = specific weight, lb/ft³

Subscripts

aw = adiabatic wall
c = coolant
l = local (just outside of boundary layer)
0 = zero injection or uncooled case
w = wall
w, air = air at wall temperature

Introduction

MASS injection, either by ablation or transpiration, can reduce the net heat transfer from the hot-gas stream in the boundary layer to the surface by an appreciable amount. In addition, mass injection at a leading edge or stagnation point offers protection to surfaces downstream by the film-cooling process. In the past, numerous ground tests have been conducted employing these cooling systems. Since the simulation of actual flight conditions in ground facilities is seldom achieved (e.g., duplicating the conditions a spacecraft would encounter upon re-entering the earth's atmosphere at supercircular velocities), the NASA Langley Research Center initiated a flight-test research program that would provide information in an actual flight environment.

Presented at the AIAA/ASD Vehicle Design and Propulsion Meeting, Dayton, Ohio, November 4–6, 1963; revision received April 20, 1964.

* Aerospace Engineer, Applied Materials and Physics Division.
† Aerospace Engineer, Applied Materials and Physics Division; presently Director of Advanced Programs, Emerson Electric Company, St. Louis, Mo.
‡ Aerospace Engineer, Applied Materials and Physics Division. Member AIAA.

The investigations were conducted employing solid-fuel rocket-propelled vehicle systems. The number of rocket stages used varied from three to five depending on the performance required for each individual experiment. One of the vehicle systems utilized the NASA-developed Scout booster.

The results of several free-flight investigations, covering an altitude range from 177,000 to 25,000 ft and peak velocities of 3900 to 22,200 fps, are discussed. Thermal protection in these experiments was provided either by subliming ablators or by transpiration cooling. Furthermore, it is shown how the material effectiveness of subliming ablators may be determined, simply and directly, from transpiration cooling results. This permits direct comparison between the two types of heat protection and, more significantly, allows extrapolation, based on low-speed transpiration data, of ablation material effectiveness to supercircular velocities.

Models

A typical model design used to investigate both transpiration and downstream cooling is shown in Fig. 1. The particular configuration shown is a solid conical body having a blunt nose cap made of porous stainless steel. Nitrogen gas is released from the accumulator at a predetermined time during the flight test. The nitrogen coolant flow rate is determined from measurements of the pressure differential across the porous nose and the pressure and temperature of the gas in the nose chamber. Thermocouples are spot-welded to the inner surface of the porous nose cap and of the conical afterbody to measure the heat transfer with coolant injection through the porous nose.

A typical Teflon ablation model, instrumented with variable-capacitance ablation rate sensors,[1] is shown in Fig. 2. The variable-capacitance ablation rate sensor which continuously measures the ablation rate of Teflon was developed by NASA; it is shown in Fig. 3.

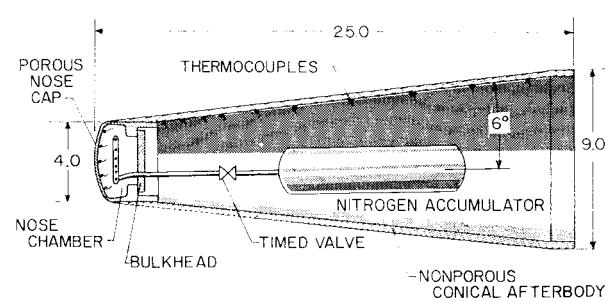

Fig. 1 Transpiration and downstream cooling model.

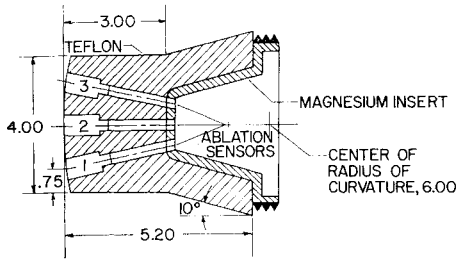

Fig. 2 Typical ablation model.

Test Regime

Figure 4 shows that the flight-test regime covered altitudes from 25 to 177 kft and peak velocities from 3.9 to 22.2 kft/sec. The corresponding enthalpy range was approximately 190 to 10,000 Btu/lb; dynamic pressure varied from 100 to 7000 psf and freestream Reynolds number per foot varied from 0.5×10^6 to 6×10^6. In addition, several ground tests were conducted in a Mach 2.0, ethylene-heated air jet, in which Re/ft varied from about 12×10^6 at a stagnation enthalpy of 250 Btu/lb to 2×10^6 at a stagnation enthalpy of 800 Btu/lb, and the dynamic pressure was ~5200 psf.

Transpiration Cooling Results and Analysis

The results of two flight tests and a number of ground tests[2, 3] on transpiration cooling are summarized in Fig. 5, in which the shielding effect ratio, $N_{St}/N_{St,0}$, is expressed as a function of the nondimensional flow-rate parameter $(F/N_{St,0})(c_{p,c}/c_{p,l})(T_l/T_w)^n$. The lower curve (dashed region) shows free-flight results[2] to a maximum velocity of 10,400 fps for large rates of nitrogen flow. Also shown is the theoretical curve[4] (solid) for relatively moderate rates of mass injection into a three-dimensional laminar stagnation boundary layer. The theoretical results of Ref. 4 were for values of T_l/T_w ranging from $\frac{1}{4}$ to 4; however, the results were correlated by including the temperature ratio in the nondimensional flow-rate parameter with n equal to 0.21. This technique, introduced in Ref. 5, permits transpiration data with values of $T_l/T_w \neq 1$ to be plotted on a single curve. The flight data[2] with large rates of mass injection correlate well with the theory for relatively moderate rates when $(T_l/T_w)^{0.21}$, which varies from 1.45 to 1.66, is included in the nondimensional flow-rate parameter. Examination of the flight data shows a significant heat-transfer reduction because of transpiration cooling.

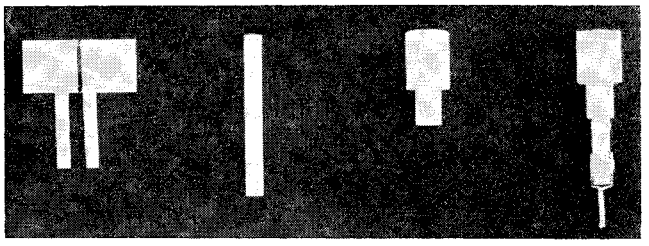

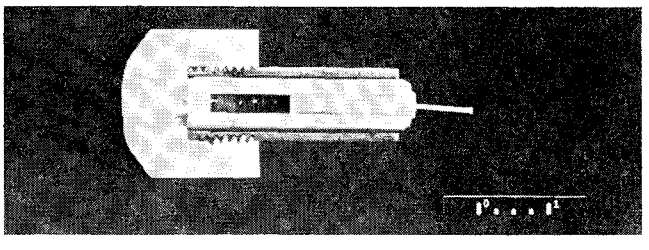

Ablation sensor installed in Teflon ablation probe

Fig. 3 Details of ablation sensor.

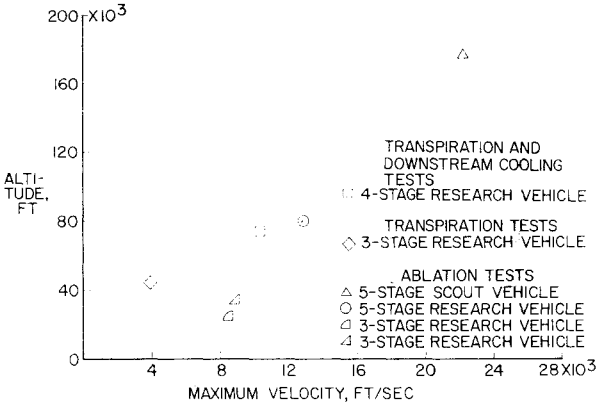

Fig. 4 Test regime.

The upper curve of Fig. 5 represents the theoretical results for a turbulent boundary layer computed from the relation (obtained from Ref. 6 for $T_l/T_w = 1$):

$$\frac{N_{St}}{N_{St,0}} = \frac{(F/N_{St,0})(c_{p,c}/c_{p,l})}{\exp[(F/N_{St,0})(c_{p,c}/c_{p,l})] - 1}$$

Turbulent results[3] for free flight to a maximum velocity of 3910 fps and for Mach 2.0 ground tests were correlated by including the temperature ratio in the nondimensional flow-rate parameter, with $n = 1.3$.

Figure 6 shows the downstream cooling temperature parameter $(T_w - T_c)/(T_{aw} - T_c)$ as a function of the flow-rate parameter $F_\xi c_{p,c}/N_{St,0} c_{p,l}$ for two tests. The nondimensional coolant flow rate F_ξ was computed from $F_\xi = w/S(\rho V)_l$, where w was the flow rate of coolant and S was the cooled area downstream of the porous nose. The center curve shows free-flight results[2] to a maximum velocity of 6020 fps for a laminar boundary layer with a zero pressure gradient. The upper curve represents data[7] for a turbulent, zero-pressure-gradient boundary layer in a Mach 2.0 ground-test facility. Comparison of the two curves indicates that, for the same coolant flow rate, lower surface temperatures are achieved in a laminar boundary layer with downstream cooling. The lower theoretical curve shown in Fig. 6 shows that a completely porous wall in a turbulent boundary layer[6] would give still lower wall temperatures. Under certain conditions, however, it is possible to maintain solid surfaces at a safe temperature level and use less coolant with a downstream cooling system, since the maximum allowable temperatures of porous materials are generally a great deal lower than for solid materials. The accuracy of both the transpiration and downstream cooling test results was estimated to be within 5%.

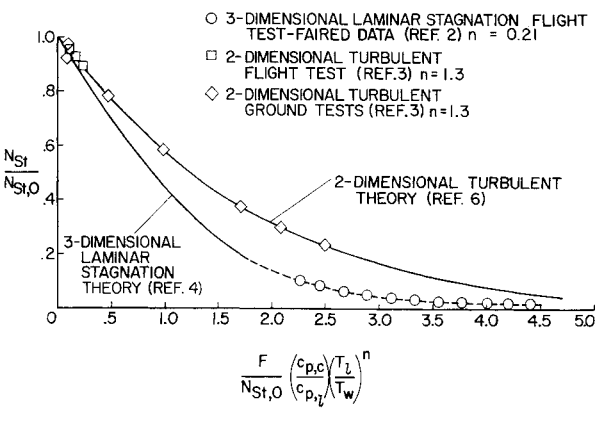

Fig. 5 Transpiration test results.

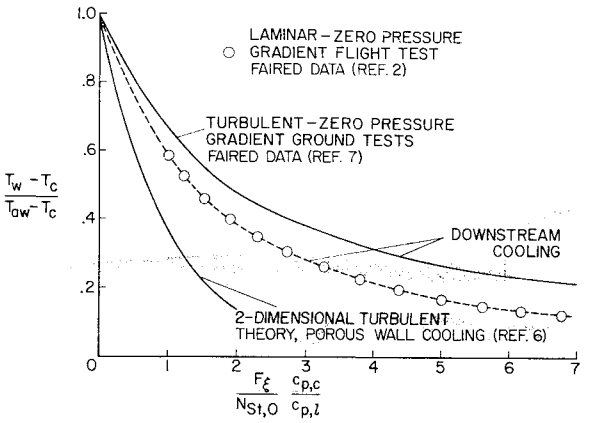

Fig. 6 Downstream cooling test results compared with porous wall cooling.

Ablation Results and Analysis

The effectiveness of subliming ablation materials can be derived simply and directly from transpiration cooling results, since the cooling mechanism of this category of ablation materials is analogous to transpiration cooling. Once the relationship between

$$\frac{N_{St}}{N_{St,0}}$$

and

$$\frac{F}{N_{St,0}} \frac{c_{p,c}}{c_{p,l}} \left(\frac{T_l}{T_w}\right)^n$$

is known from transpiration data, the effective heat of ablation h_{eff} can be determined. The transformation relationships[5] are

$$\frac{h_{eff}}{h_{ov}} = \frac{N_{St,0}}{N_{St}} \tag{1}$$

$$\frac{f(H_{aw} - H_{w,air})}{h_{ov}} \left(\frac{c_{p,c}}{c_{p,l}}\right)\left(\frac{T_l}{T_w}\right)^n = \frac{(F/N_{St,0})(c_{p,c}/c_{p,l})(T_l/T_w)^n}{(N_{St}/N_{St,0})} \tag{2}$$

Hence, h_{eff} can be obtained in terms of the enthalpy difference across the boundary layer $(H_{aw} - H_{w,air})$ and h_{ov}, the intrinsic heat capacity of the material, which is defined as the absorbing capacity of a material prior to ablation. The factor f is the fraction of melt that vaporizes for a melting-vaporizing ablation material. For the present results, f is equal to 1.0, since this paper deals only with subliming ablators. However, the foregoing relationships should also apply to materials in the melting-vaporizing class upon inclusion of the pertinent material property values. The inclusion of $c_{p,c}/c_{p,l}$ in Eq. (2) permits shielding results for any coolant

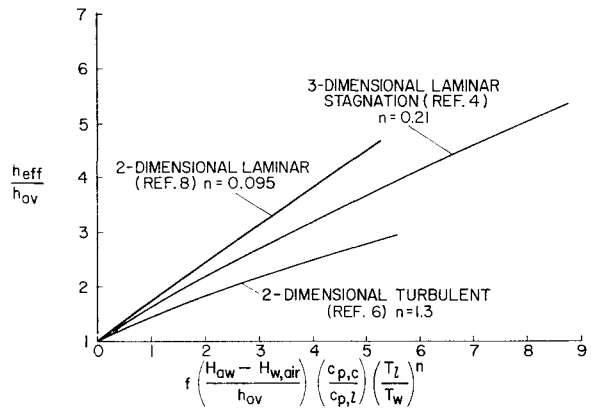

Fig. 7 Effective heat of ablation as a function of enthalpy parameter for several boundary-layer types.

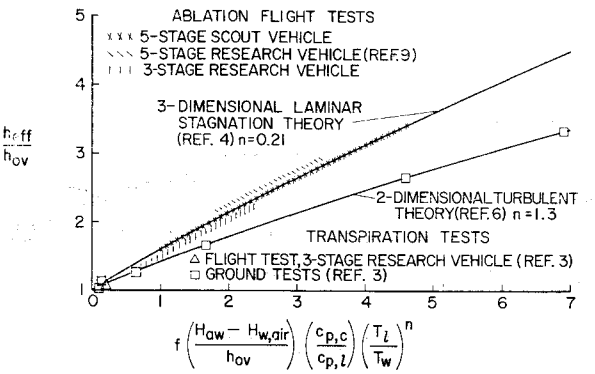

Fig. 8 Effective heat of ablation as a function of enthalpy potential.

to be used in the transformation. Furthermore, the inclusion of $(T_l/T_w)^n$ permits shielding results with any temperature ratio to be used, where n varies according to the boundary-layer type. Figure 7 shows effective-heat-of-ablation results obtained from theoretical transpiration data of Refs. 4, 6, and 8 for several boundary-layer types.

Figure 8 shows theoretical curves for the effective heat of ablation vs the enthalpy parameter for a three-dimensional laminar stagnation boundary layer and for a turbulent zero-pressure-gradient boundary layer, shown previously in Fig. 5, together with results from four ablation flight tests. The ablation flight test data in Fig. 8 are from Ref. 9 and unpublished experiments conducted at the NASA Langley Research Center. The velocity variation covered by the flight tests was from approximately 5000 to 22,200 fps. The values of h_{eff} for the ablation tests were computed from the relation

$$h_{eff} = q_0/\dot{m}$$

where q_0 is the heat transfer to a nonablating surface having the same temperature as the ablating surface. The value of h_{ov} used was 900 Btu/lb for Teflon. All of the experimental ablation results are seen to correlate with theory for a three-dimensional laminar stagnation boundary layer; for purposes of clarity, however, some of the ablation test data have been displaced from the theory curve. The accuracy of the ablation test results was estimated to be within 5%.

Figure 9 shows the extension of ablation cooling effectiveness to high speeds from low-speed transpiration data.[2] Also shown are the ablation flight tests, along with theory for a three-dimensional laminar stagnation boundary layer. Since the value of the enthalpy parameter from transformed transpiration data is proportional to the mass injection rate, large rates of mass injection for a transpiration test would simulate a high flight velocity for an ablation test wherein the mass injection rates are relatively low. Although the maximum velocity for the transpiration flight test[2] was only 10,400 fps, since large rates of mass injection were used, the trans-

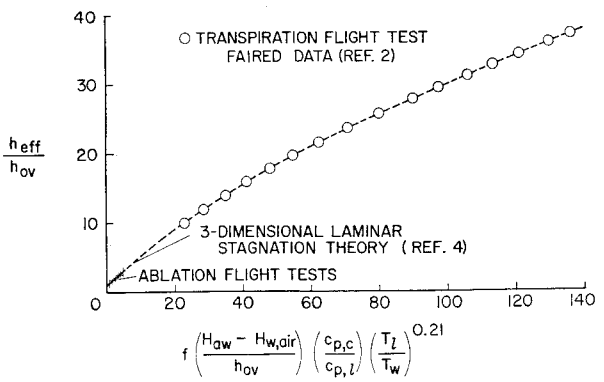

Fig. 9 Extension of ablation cooling effectiveness to high speeds from low-speed transpiration test.

formed results permit an extension of theory to supercircular velocities. The ablation flight-test results at velocities up to 22,200 fps are in good agreement with the technique of predicting the cooling effectiveness of subliming ablators. However, further testing in the higher velocity regime is required to verify further the predictions.

Conclusions

The following conclusions are based on the results of several free-flight investigations wherein the thermal protection was provided by either a subliming ablator or by transpiration cooling: 1) The analogous behavior of subliming ablators to transpiration cooling permits direct comparison of these two types of heat protection; and 2) since the effectiveness of ablating materials is proportional to the mass injection rate and the vehicle velocity, extrapolation of the transpiration cooling effect based on relatively low-speed transpiration data, wherein high mass ejection rates were used, permits the prediction of material effectiveness to supercircular speeds.

References

[1] Winters, C. W. and Bracalente, E. M., "A sensor for obtaining ablation rates," NASA TN D-800 (1961).

[2] Walton, T. E., Jr., "Free-flight investigation of mass transfer cooling on a blunt cone to a Mach number of 10.6," NASA TN D-2197 (1964).

[3] Walton, T. E., Jr. and Rashis, B., "Measurement and empirical correlation of transpiration cooling parameters on a 25° cone in a turbulent boundary layer in both free flight and a hot-gas jet," NASA TN D-967 (1961).

[4] Howe, J. T. and Mersman, W. A., "Solutions of the laminar compressible boundary-layer equations with transpiration which are applicable to the stagnation regions of axisymmetric blunt bodies," NASA TN D-12 (1959).

[5] Rashis, B. and Hopko, R. N., "An analytical investigation of ablation," NASA TM X-300 (1960).

[6] Leadon, B. M. and Scott, C. J., "Measurement of recovery factors and heat transfer coefficients with transpiration cooling in a turbulent boundary layer at $M = 3.0$ using air and helium as coolants," Institute of Technology, Aeronautical Engineering Dept., Univ. of Minnesota Research Rept. 126(Contract AF 18(600)-1226) (February 1956).

[7] Witte, W. G. and Rashis, B., "An experimental investigation and correlation of the heat reduction to nonporous surfaces behind a porous leading edge through which coolant is ejected," NASA TM X-235 (1960).

[8] Brown, W. B. and Donoughe, P. L., "Tables of exact laminar-boundary-layer solutions when the wall is porous and fluid properties are variable," NACA TN 2479 (1951).

[9] Winters, C. W., Witte, W. G., Rashis, B., and Hopko, R. N., "Free-flight investigation of ablation of a blunt body to a Mach number 13.1," NASA TN D-1500 (1962).

SEPTEMBER-OCTOBER 1964 J. SPACECRAFT VOL. 1, NO. 5

Thermal Radiation from the Exhaust Plume of an Aluminized Composite Propellant Rocket

S. J. Morizumi* and H. J. Carpenter*
TRW Space Technology Laboratories, Redondo Beach, Calif.

A technique is developed for calculating rocket base heating and spacecraft heating environments due to particle radiation from a single nozzle exhaust plume. It has successfully predicted experimental results. The analysis treats radiation from a cloud of particles as that from an equivalent radiating surface. Thus, the problem is reduced to the determination of the proper values of the apparent surface emissivity and the effective temperature. In defining the apparent emissivity, an analogy with neutron scattering for a cylindrical cloud is adopted which shows the apparent emissivity to be dependent on particle emissivity and cloud optical thickness. Since the plume is nonuniform in particle size, concentration, and temperature, certain averaging techniques are used to define mean values of optical thickness and temperature. The particle flow-field information (particle concentrations, temperatures, and trajectories) necessary to determine these two quantities is provided by a two-phase flow-field computer program.

Nomenclature

a = $2\pi r_p/\lambda$
E = photon (radiant energy) flux, Btu/ft²-sec
F = shape factor from unshaded portion of particle plume to a surface element
I = radiant intensity, Btu/ft²-sec-sr-μ
k = cosine distribution exponent, Eq. (7)
L = total length of path across a particle plume, ft
L_0 = distance along view path from a surface element to particle plume boundary, ft
l = length through a particle plume, ft
m = number of plume segments
N = particle concentration, particles/ft³
$P_{i-1,k}$ = collision probability, Eq. (2)
P_n $\equiv P_{n,k}$
p_c = rocket chamber pressure, psia
p_e = ambient pressure, psia
Q = efficiency factor, Eq. (23)
$\dot{q}$ = radiant heat-transfer rate, Btu/ft²-sec
r = particle radius, ft or μ
T = absolute temperature, °R
x = distance along path from boundary of a particle cloud, ft

Presented as Preprint 64-61 at the AIAA Aerospace Sciences Meeting, New York, January 20–22, 1964; revision received March 31, 1964. The authors wish to express appreciation for the helpful discussions held with numerous members of the Space Technology Laboratories Technical Staff, and particularly for the computational assistance provided by Fern R. Bright and Mary L. Persons.

* Member of the Technical Staff. Member AIAA.